JOURNAL OF AIRCRAFT
Vol. 36, No. 1, January–February 1999

Structural Optimization with Thermal and Mechanical Constraints

Suqiang Xu* and Ramana V. Grandhi†
Wright State University, Dayton, Ohio 45435

This paper reports on the testing of the adaptability of the new approximation tools for thermal structural optimization. A finite element based procedure is proposed for obtaining a minimum mass design of structures subjected to stress, displacement, and temperature constraints. The optimization is based on a new two-point approximation method for the function. The coupling between thermal and structural sensitivities is taken into account to ensure the convergence. The direct or adjoint method is used for the sensitivity analysis. The two-point approximation is the incomplete second-order Taylor series expansion in terms of the intervening variables. The exponent of each design variable and the unknown constant in the second-order terms can be obtained in a closed form. This two-point approximation is used for temperature, displacement, and internal force approximations. Stress constraints are calculated by using approximated internal forces. Finally, the optimization procedure is demonstrated by two examples: the first example is the design of a titanium plate with aluminum bars and the second example is a structural wing box. These examples are subjected to external heating and mechanical loads, with temperature, strength, and minimum gauge constraints.

Introduction

STRUCTURAL design of flight vehicles that travel through the Earth's atmosphere, either to or from space or in sustained flight conditions, poses a challenge to structural engineers. One of the major challenges is to design structures and select materials that are able to withstand the aerothermal loads of high-speed flight.[1]

The design of a high-speed structure must satisfy mechanical and thermal design requirements. Mechanical requirements must be satisfied to ensure structural integrity, which imposes limits on stresses, displacements, frequencies, and other constraints. Thermal requirements must be satisfied to avoid material property degradation and excessive temperatures in cargo and crew compartments, which imposes upper limits on structural temperatures.

Two major solution approaches for thermostructural system optimization are optimizations based on a continuum system and a discrete model. The continuum-based method is mainly concentrated on applications involving the shape sensitivity analysis. Meric[2] and Aithal and Saigal[3] used the boundary element method for sensitivity analysis of thermoelastic or thermal problems. Dems[4] derived boundary sensitivity expressions for themoelasticity solids. Hou et al.[5] used a domain method for sensitivity analysis and optimization of themoelastic solids. Yang[6] presented shape design sensitivities of thermoelasticity problems by using the material derivative approach. Tortorelli et al.[7] and Pangiotis and Tortorelli[8] derived analytical sensitivities for nonlinear dynamic or transient systems. The continuum sensitivities and related optimization methods were mainly used for local component shape designs. Reference 8 contains an extensive list of publications in the area of thermomechanical optimization using the continuum sensitivity analyses.

Received Aug. 24, 1997; revision received June 3, 1998; accepted for publication Aug. 9, 1998. This paper is declared a work of the U.S. Government and is not subject to copyright protection in the United States.

*Research Associate, Department of Mechanical and Materials Engineering. Member AIAA.

†Distinguished Professor, Department of Mechanical and Materials Engineering. Associate Fellow AIAA.

This paper aims at the size optimization of large-scale thermal structures. The discrete sensitivity and optimization method are usually applied to this kind of problem. More details on the review of this field are provided because of its close relation to this paper.

Haftka and Markus[9] considered three thermal sensitivity analysis methods. The first method requires calculation of the derivatives of the entire temperature field. The second method requires the calculation of a constraint-dependent adjoint field. The third method is the finite differences approach. It was shown that the choice of the most efficient technique depends on the ratio of the number of temperature constraints to the number of design variables, as well as the thermal analysis method employed. Haftka and Markus[10] explored two avenues to enhance the effectiveness of the finite difference approach to calculating derivatives of temperatures and thermal constraints. The first avenue was the simultaneous solution of temperatures and their derivatives. The second avenue was the optimal selection of the magnitude of the perturbations of the design variables.

Usually, structural syntheses were concentrated on designing structures under mechanical loads for mechanical requirements. Thermal loads were incorporated as specified structural temperatures supplied by an independent thermal analysis; equivalent loads were added to the applied mechanical loads.[11] The temperature was entered into the optimization problem indirectly through the strength requirements; thus, explicit thermal requirements were not included. The temperatures of grids on the structures were not recalculated as the structure was resized. Thus, good initial estimates of the structural member sizes were required to avoid significant differences between the temperature distributions in the initial and final designs. A logical improvement to the existing thermal/structural design methods is the incorporation of temperature constraints and the recalculation of temperatures during resizing. Adelman et al.[12] and Adelman and Sawyer[13] solved coupled thermal/structural optimization directly by applying the sequence of unconstrained minimization techniques and optimality criteria algorithms. Haftka and Shore[14] presented two approximation concepts for combined thermal/structural design. The first concept was approximate thermal analysis based on the first derivatives of structural temperatures with respect to design variables. The second concept was the use of a critical time point

for combined thermal and stress analysis of structures with transient loading conditions. Haftka[15] applied the approximation concepts to the combined thermal/structural design procedure in which the temperature was approximated first. A subproblem was then formed using the approximate thermal analysis and actual structural analysis. This subproblem was solved using the approximation concepts. After the design converged for this subproblem, another thermal analysis was performed and the cycle was repeated. Convergence was achieved when the final approximate temperature distribution was close to the actual temperature. This approach includes two loops; the outer loop corresponds to the temperature approximation, whereas the inner loop performs structural optimization under a given approximate temperature distribution.

Thomas and Shyy[16] studied the influence of thermal sensitivities on structural response sensitivities. They concluded that it is not practical to assume a constant temperature distribution throughout the optimization process. The coupling between the steady-state heat transfer problem and structural analysis could be strong. That means that the effect of design changes on the thermal loads should be taken into account, or poor convergence characteristics may result.

Thermal loads are presently involved in the design applications[17–22] and the multidisciplinary optimization software systems,[11,23–29] where temperatures usually enter the design as the variable-independent inputs. Cheu[17,18] attempted to develop an efficient procedure for sensitivity analysis in the shape optimization of axisymmetric structures and applied the technique to the optimal design of gas-turbine disks subjected to thermomechanical loading. Hattori and Ohnishi[19] used the sequential linear programming to optimize rotational wheel shape under transient thermal and centrifugal loading. Shao and Guan[20] reduced the maximum of transient thermal stress level of a nuclear pressure vessel during startup and shutdown processes by using the recursive quadratic programming method. Ke[21] introduced a rule-based geometric approach to the form optimization of axisymmetric components with transient thermoelastic loading. Programmed geometric rules were used to iteratively modify the shape. Autio[22] tailored the behavior of a laminated plate with given boundary temperatures and displacement constraints by varying the orientation of the reinforcement in the different layers. References 23–29 described different multidisciplinary design optimization software systems for different structural backgrounds in which the temperature was one of the loads.

Existing commercial packages such as ASTROS[30] and GENESIS[16,31] usually deal with temperatures as loads instead of as constraints. Temperatures enter the optimization procedure as variable-independent inputs in ASTROS,[30] in which heat transfer analysis is not needed during the design iteration. GENESIS[16] takes into account the dependence of temperatures on variables in which temperatures are obtained by heat transfer analysis during the design iteration.

Compared with structural optimization with mechanical loads, studies about thermal structural optimization are relatively limited, particularly for the optimization under temperature and mechanical constraints at the same time.

In this work, a finite element based procedure is described for obtaining a minimum mass design of structures subjected to stress, displacement, and thermal constraints. This procedure is based on mathematical programming using the approximation concept. A new two-point approximation (TANA-3)[32] for a function is used for the behavioral constraints that include temperature, displacement, and stress limits. For stress constraints, internal forces are approximated first and then stresses are calculated by the approximated forces. Unlike Haftka's previous work,[15] temperature, displacement, and stress constraints are simultaneously approximated in this new procedure. A subproblem is formed with all types of approximated responses. The coupling between thermal and structural sensitivities is taken into account.

Problem Statement

Problem Definition

The thermal structural optimization problem with stress, displacement, and temperature constraints is mathematically stated as follows:

$$\text{Min} \quad W(\boldsymbol{X}) \tag{1}$$

$$\text{subject to} \quad T_i/\bar{T}_i - 1 \leq 0, \qquad i = 1, \ldots, nn \tag{2}$$

$$U_i/\bar{U}_i - 1 \leq 0, \qquad i = 1, \ldots, nn \tag{3}$$

$$\sigma_i/\bar{\sigma}_i - 1 \leq 0, \qquad i = 1, \ldots, ne \tag{4}$$

$$\boldsymbol{X}^L \leq \boldsymbol{X} \leq \boldsymbol{X}^U \tag{5}$$

Where, $W(\boldsymbol{X})$ is the structural weight; $\boldsymbol{X}$ is the design variable vector that includes areas of rod elements, thicknesses of membrane elements; T_i, $\bar{T}_i$, U, $\bar{U}_i$ are, respectively, temperature, temperature limit, displacement, and displacement limit of the ith node; σ_i, $\bar{\sigma}_i$ are equivalent stress (such as von Mises stress) at an interested point and stress limit; nn is number of nodes; ne is number of elements; and $\boldsymbol{X}^L$, $\boldsymbol{X}^U$ are the lower and upper bounds of $\boldsymbol{X}$, respectively. Multiple load conditions can be considered. The temperature is expected to have a higher nonlinearity with respect to design variables than the displacement. This is because the nodal heat loads are dependent on design variables, whereas the nodal force vector is usually independent of the design variables.

Temperature Analysis

Structural temperatures are calculated using a finite element analysis. The equation for calculating temperatures is

$$C\boldsymbol{T} = \boldsymbol{Q} \tag{6}$$

where C is a conductivity matrix; $\boldsymbol{T}$ is a vector of unknown temperatures, and its elements are T_i; and $\boldsymbol{Q}$ is an applied thermal load vector including contributions from convective heating and prescribed heat flux.

Structural Analysis

The static structural analysis problem to be solved using the finite element method can be stated as

$$K\boldsymbol{U} = \boldsymbol{P} \tag{7}$$

where K is the global stiffness matrix; $\boldsymbol{U}$ is the vector of grid point displacements, and $\boldsymbol{P}$ is the vector of nodal loads. The global stiffness matrix is assembled from the element stiffness matrices that are formulated as

$$K^e = \int_v B^T D B \, dV \tag{8}$$

where B is the strain-displacement matrix and D is the stress–strain matrix. The elemental nodal loads caused by a thermal load are

$$P^e = \int_v B^T D \boldsymbol{a} (T - T_0) \, dV \tag{9}$$

where T is the element temperature, T_0 is the stress-free temperature, and $\boldsymbol{a}$ is the vector of thermal expansion coefficient for the element.

After the nodal displacements are determined using Eq. (7), the element stresses at any point can be calculated using

$$\boldsymbol{\sigma} = D[BU - \boldsymbol{a}(T - T_0)] \tag{10}$$

where B and T are calculated at the point of interest (usually the center of the element).

New Two-Point Approximation

The previous two-point approximations[33,34] have either incomplete matching at two data points or the additional solving of equations are needed to obtain some parameters. The previous two-point adaptive nonlinear approximations were called TANA-1 and TANA-2. The present two-point approximation (TANA-3)[32] is the incomplete second-order Taylor series expansion in terms of the intervening variables, in which the Hessian matrix is diagonal and changeable. The exponent of each design variable and the unknown constant on the second-order terms are evaluated by matching the derivatives and value of the approximate function with the previous data-point gradients and the value of the original function, respectively. All unknowns are identified in closed forms. Both the function and gradient of the two-point approximation are equal to those of the original function at two data points. Because this method is a natural evolution from the previous two methods, it is called as TANA-3. This two-point approximation is applied to temperature, displacement, and internal force approximations in the present work.

The function $F(\boldsymbol{Y})$ can be expanded with respect to the intervening variable $Y_i = X_i^{p_i}$, as

$$\tilde{F}(\boldsymbol{X}) = F(\boldsymbol{X}_2) + \sum_{i=1}^{n} \frac{\partial F(\boldsymbol{X}_2)}{\partial X_i} \frac{X_{i,2}^{1-p_i}}{p_i} (X_i^{p_i} - X_{i,2}^{p_i}) + \frac{1}{2}\varepsilon(\boldsymbol{X}) \sum_{i=1}^{n} (X_i^{p_i} - X_{i,2}^{p_i})^2 \tag{11}$$

specifying

$$\varepsilon(\boldsymbol{X}) = H \Big/ \left[\sum_{i=1}^{n} (X_i^{p_i} - X_{i,1}^{p_i})^2 + \sum_{i=1}^{n} (X_i^{p_i} - X_{i,2}^{p_i})^2 \right] \tag{12}$$

where p_i and H are constants to be determined based on the information of the previous point. It will be shown that $\varepsilon(\boldsymbol{X})$ would uncouple p_i and H in the equations to compute them, which will make them easier to calculate.

Differentiating Eq. (11)

$$\frac{\partial \tilde{F}(\boldsymbol{X})}{\partial X_i} = \left(\frac{X_i}{X_{i,2}}\right)^{p_i - 1} \frac{\partial F(\boldsymbol{X}_2)}{\partial X_i} + E(\boldsymbol{X}) \tag{13}$$

where

$$E(\boldsymbol{X}) = \left\{ H p_i X_i^{p_i - 1} \left[(X_i^{p_i} - X_{i,2}^{p_i}) \sum_{j=1}^{n} (X_j^{p_j} - X_{j,1}^{p_j})^2 - (X_i^{p_i} - X_{i,1}^{p_i}) \sum_{j=1}^{n} (X_j^{p_j} - X_{j,2}^{p_j})^2 \right] \right\} \Big/ \left[\sum_{j=1}^{n} (X_j^{p_j} - X_{j,1}^{p_j})^2 + \sum_{j=1}^{n} (X_j^{p_j} - X_{j,2}^{p_j})^2 \right]^2 \tag{14}$$

It can be noticed that $E(\boldsymbol{X})$ diminishes to zero at two data points. That is

$$E(\boldsymbol{X}_1) = E(\boldsymbol{X}_2) = 0 \tag{15}$$

So

$$\frac{\partial \tilde{F}(\boldsymbol{X}_2)}{\partial X_i} = \frac{\partial F(\boldsymbol{X}_2)}{\partial X_i} \tag{16}$$

$$\frac{\partial \tilde{F}(\boldsymbol{X}_1)}{\partial X_i} = \left(\frac{X_{i,1}}{X_{i,2}}\right)^{p_i - 1} \frac{\partial F(\boldsymbol{X}_2)}{\partial X_i} \tag{17}$$

It is easy to show that the second-order term of Eq. (11) is zero at the current point $\boldsymbol{X}_2$, and is $0.5H$ at the previous point $\boldsymbol{X}_1$. So

$$\tilde{F}(\boldsymbol{X}_2) = F(\boldsymbol{X}_2) \tag{18}$$

$$\tilde{F}(\boldsymbol{X}_1) = F(\boldsymbol{X}_2) + \sum_{i=1}^{n} \frac{\partial F(\boldsymbol{X}_2)}{\partial X_i} \frac{X_{i,2}^{1-p_i}}{p_i} (X_{i,1}^{p_i} - X_{i,2}^{p_i}) + \frac{1}{2} H \tag{19}$$

From Eqs. (16) and (18). It is shown that the function and derivative values of the approximation match with the exact ones at $\boldsymbol{X}_2$. $n + 1$ uncoupled equations are obtained by matching the derivative and function values with the previous point, $\boldsymbol{X}_1$

$$\frac{\partial F(\boldsymbol{X}_1)}{\partial X_i} = \left(\frac{X_{i,1}}{X_{i,2}}\right)^{p_i - 1} \frac{\partial F(\boldsymbol{X}_2)}{\partial X_i}, \qquad i = 1, \ldots, n \tag{20}$$

$$F(\boldsymbol{X}_1) = F(\boldsymbol{X}_2) + \sum_{i=1}^{n} \frac{\partial F(\boldsymbol{X}_2)}{\partial X_i} \frac{\partial X_{i,2}^{1-p_i}}{p_i} (X_{i,1}^{p_i} - X_{i,2}^{p_i}) + \frac{1}{2} H \tag{21}$$

From Eq. (20) and Eq. (21), p_i and H are obtained in a closed-form solution as follows:

$$p_i = 1 + \ell n \left[\frac{\partial F(\boldsymbol{X}_1)}{\partial X_i} \Big/ \frac{\partial F(\boldsymbol{X}_2)}{\partial X_i} \right] \Big/ \ell n \left(\frac{X_{i,1}}{X_{i,2}} \right) \tag{22}$$

$$H = 2 \left[F(\boldsymbol{X}_1) - F(\boldsymbol{X}_2) - \sum_{i=1}^{n} \frac{\partial F(\boldsymbol{X}_2)}{\partial X_i} \frac{X_{i,2}^{1-p_i}}{p_i} (X_{i,1}^{p_i} - X_{i,2}^{p_i}) \right] \tag{23}$$

When $\partial F(\boldsymbol{X}_1)/\partial X_i / \partial F(\boldsymbol{X}_2)/\partial X_i$ or $X_{i,1}/X_{i,2}$ is less than zero, or when other computational problems arise in Eq. (22), a specialized value to p_i, i.e., 1 or -1, is assigned. For example, consider the optimization iterations near the convergence domain. The variables barely change, and so $X_{i,1}/X_{i,2}$ is close to 1. In this situation, one can assign $p_i = 1$ or -1. On the other side, the absolute value of p_i calculated in Eq. (22) may be very large and subsequently deteriorate the approximation. Bound $p_{\max}$ is put on p_i. When p_i is less than $-p_{\max}$ or greater than $p_{\max}$, it is rounded up to $-p_{\max}$ or down to $p_{\max}$. For examples in this paper, $p_{\max} = 5$ is taken.

Constraint Approximations

Temperature and Displacement Approximation

Temperature and displacement are approximated by using Eq. (11)

$$\tilde{T}(\boldsymbol{X}) = T(\boldsymbol{X}_2) + \sum_{i=1}^{n} \frac{\partial T(\boldsymbol{X}_2)}{\partial X_i} \frac{X_{i,2}^{1-p_i}}{p_i} (X_i^{p_i} - X_{i,2}^{p_i}) + \frac{1}{2}\varepsilon(\boldsymbol{X}) \sum_{i=1}^{n} (X_i^{p_i} - X_{i,2}^{p_i})^2 \tag{24}$$

$$\tilde{U}(\boldsymbol{X}) = U(\boldsymbol{X}_2) + \sum_{i=1}^{n} \frac{\partial U(\boldsymbol{X}_2)}{\partial X_i} \frac{X_{i,2}^{1-p_i}}{p_i} (X_i^{p_i} - X_{i,2}^{p_i}) + \frac{1}{2}\varepsilon(\boldsymbol{X}) \sum_{i=1}^{n} (X_i^{p_i} - X_{i,2}^{p_i})^2 \tag{25}$$

Force Approximation

In this work, the force at the center of each element is approximated. This way, the approximate value of the stress constraint is recovered. Therefore, the quality of the constraint approximation is improved.

For the rod element

$$\tilde{F}(\boldsymbol{X}) = F(\boldsymbol{X}_2) + \sum_{i=1}^{n} \frac{\partial F(\boldsymbol{X}_2)}{\partial X_i} \frac{X_{i,2}^{1-p_i}}{p_i} (X_i^{p_i} - X_{i,2}^{p_i}) + \frac{1}{2}\varepsilon(\boldsymbol{X}) \sum_{i=1}^{n} (X_i^{p_i} - X_{i,2}^{p_i})^2 \tag{26}$$

$$\sigma = \tilde{F}(\boldsymbol{X})/A \tag{27}$$

For the membrane element, the internal force vector $\boldsymbol{N} = (N_x, N_y, N_{xy})$ is approximated.

$$\tilde{N}_x(\boldsymbol{X}) = N_x(\boldsymbol{X}_2) + \sum_{i=1}^{n} \frac{\partial N_x(\boldsymbol{X}_2)}{\partial X_i} \frac{X_{i,2}^{1-p_i}}{p_i} (X_i^{p_i} - X_{i,2}^{p_i}) + \frac{1}{2}\varepsilon(\boldsymbol{X}) \sum_{i=1}^{n} (X_i^{p_i} - X_{i,2}^{p_i})^2 \tag{28}$$

$$\tilde{N}_y(\boldsymbol{X}) = N_y(\boldsymbol{X}_2) + \sum_{i=1}^{n} \frac{\partial N_y(\boldsymbol{X}_2)}{\partial X_i} \frac{X_{i,2}^{1-p_i}}{p_i} (X_i^{p_i} - X_{i,2}^{p_i}) + \frac{1}{2}\varepsilon(\boldsymbol{X}) \sum_{i=1}^{n} (X_i^{p_i} - X_{i,2}^{p_i})^2 \tag{29}$$

$$\tilde{N}_{xy}(\boldsymbol{X}) = N_{xy}(\boldsymbol{X}_2) + \sum_{i=1}^{n} \frac{\partial N_{xy}(\boldsymbol{X}_2)}{\partial X_i} \frac{X_{i,2}^{1-p_i}}{p_i} (X_i^{p_i} - X_{i,2}^{p_i}) + \frac{1}{2}\varepsilon(\boldsymbol{X}) \sum_{i=1}^{n} (X_i^{p_i} - X_{i,2}^{p_i})^2 \tag{30}$$

$$\sigma_x = \tilde{N}_x(\boldsymbol{X})/t \tag{31}$$

$$\sigma_y = \tilde{N}_y(\boldsymbol{X})/t \tag{32}$$

$$\sigma_{xy} = \tilde{N}_{xy}(\boldsymbol{X})/t \tag{33}$$

Approximated von Mises stress is

$$\sigma = \sqrt{\sigma_x^2 + \sigma_y^2 - \sigma_x\sigma_y + 3\sigma_{xy}^2} \tag{34}$$

Sensitivity Analysis

Temperature Sensitivity

A nodal temperature can be expressed as follows:

$$T_j = \boldsymbol{V}_j^T \boldsymbol{T} \tag{35}$$

where $\boldsymbol{T}$ is the temperature vector and $\boldsymbol{V}_j$ is the virtual load vector. For temperature constraints, $\boldsymbol{V}_j$ is a unit dummy load. From Eq. (35), we get

$$\frac{\partial T_j}{\partial X_i} = \frac{\partial \boldsymbol{V}_j^T}{\partial X_i} \boldsymbol{T} + \boldsymbol{V}_j^T \frac{\partial \boldsymbol{T}}{\partial X_i} \tag{36}$$

From Eq. (6)

$$C \frac{\partial \boldsymbol{T}}{\partial X_i} + \frac{\partial C}{\partial X_i} \boldsymbol{T} = \frac{\partial \boldsymbol{Q}}{\partial X_i} \tag{37}$$

$$C \frac{\partial \boldsymbol{T}}{\partial X_i} = \left(-\frac{\partial C}{\partial X_i} \boldsymbol{T} + \frac{\partial \boldsymbol{Q}}{\partial X_i} \right) \tag{38}$$

The thermal load vector $\boldsymbol{Q}$ is dependent on design variables, so $\partial \boldsymbol{Q}/\partial X_i \neq 0$. Substituting Eq. (38) into Eq. (36) yields

$$\frac{\partial T_j}{\partial X_i} = \frac{\partial \boldsymbol{V}_j^T}{\partial X_i} \boldsymbol{T} + \boldsymbol{V}_j^T C^{-1} \left(-\frac{\partial C}{\partial X_i} \boldsymbol{T} + \frac{\partial \boldsymbol{Q}}{\partial X_i} \right) = \boldsymbol{T}^{V_j} \left(-\frac{\partial C}{\partial X_i} \boldsymbol{T} + \frac{\partial \boldsymbol{Q}}{\partial X_i} \right) \tag{39}$$

where $\boldsymbol{T}^{V_j}$ is the temperature response of the virtual load $\boldsymbol{V}_j$, that is

$$C\boldsymbol{T}^{V_j} = \boldsymbol{V}_j \tag{40}$$

$\partial C/\partial X_i$ and $\partial \boldsymbol{Q}/\partial X_i$ can easily be obtained. Therefore, the most significant part of the sensitivity analysis is to calculate the response of the virtual loads associated with the number of the near active constraints if the coupling between temperature sensitivity and structural response sensitivity is ignored [see Eqs. (43) and (44)]. Because the coupling is taken into account, every nodal temperature sensitivity is required. Under this situation, Eq. (38) should be used when the number of design variables is less than the number of degrees of freedom of the temperature.

Displacement and Force Sensitivities

Similar to the temperature sensitivity, the displacement sensitivity can be obtained as

$$\frac{\partial U_j}{\partial X_i} = \boldsymbol{e}_j^T K^{-1} \left(-\frac{\partial K}{\partial X_i} \boldsymbol{U} + \frac{\partial \boldsymbol{P}}{\partial X_i} \right) = (\boldsymbol{U}^{e_j})^T \left(-\frac{\partial K}{\partial X_i} \boldsymbol{U} + \frac{\partial \boldsymbol{P}}{\partial X_i} \right) \tag{41}$$

where $\boldsymbol{U}^{e_j}$ is the displacement response of virtual unit load $\boldsymbol{e}_j$, that is

$$K\boldsymbol{U}^{e_j} = \boldsymbol{e}_j \tag{42}$$

The node load vector includes two contributions from mechanical and thermal loads. The partial derivative of the elemental thermal load vector are as follows.

For the rod element:

$$\frac{\partial \boldsymbol{P}_j^e}{\partial X_i} = \frac{\partial A_j}{\partial X_i} \int_l B^T D\boldsymbol{a}[T(x, y, z) - T_0]\, \mathrm{d}l + A_j \int_l B^T D\boldsymbol{a} \left[\frac{\partial T(x, y, z)}{\partial X_i} \right] \mathrm{d}l \tag{43}$$

For the membrane element:

$$\frac{\partial \boldsymbol{P}_j^e}{\partial X_i} = \frac{\partial t_j}{\partial X_i} \int_A B^T D\boldsymbol{a}[T(x, y, z) - T_0]\, \mathrm{d}A + t_j \int_A B^T D\boldsymbol{a} \left[\frac{\partial T(x, y, z)}{\partial X_i} \right] \mathrm{d}A \tag{44}$$

The last term of Eqs. (43) and (44) captures the sensitivity coupling between the static analysis problem and the heat transfer problem

$$\frac{\partial T(x, y, z)}{\partial X_i} = \sum_{k=1}^{nd} N_k \frac{\partial T_K}{\partial X_i} \tag{45}$$

Where nd is the total node number per element and N_i is shape function. $\partial T_K/\partial X_i$ is obtained from Eqs. (38) or (39).

The partial derivatives of the force are as follows. For the rod element:

$$\frac{\partial F}{\partial X_i} = \frac{\partial A}{\partial X_i} D\{BU - a[T(x, y, z) - T_0]\} - ADa \frac{\partial T(x, y, z)}{\partial X_i} + ADB \frac{\partial U}{\partial X_i}$$

$$= \frac{\partial A}{\partial X_i} D\{BU - a[T(x, y, z) - T_0]\} - ADa \frac{\partial T(x, y, z)}{\partial X_i} + (U^{ADB})^T \left(-\frac{\partial K}{\partial X_i} U + \frac{\partial P}{\partial X_i} \right) \quad (46)$$

where U^{ADB} is the displacement response of the virtual load ADB, i.e.,

$$KU^{ADB} = ADB \quad (47)$$

For the membrane element:

$$\frac{\partial N}{\partial X_i} = \frac{\partial t}{\partial X_i} D\{BU - a[T(x, y, z) - T_0]\} - tDa \frac{\partial T(x, y, z)}{\partial X_i} + tDB \frac{\partial U}{\partial X_i}$$

$$= \frac{\partial t}{\partial X_i} D\{BU - a[T(x, y, z) - T_0]\} - tDa \frac{\partial T(x, y, z)}{\partial X_i} + (U^{tDB})^T \left(-\frac{\partial K}{\partial X_i} U + \frac{\partial P}{\partial X_i} \right) \quad (48)$$

where U^{tDB} is the displacement response of virtual load tDB, i.e.,

$$KU^{tDB} = tDB \quad (49)$$

Optimization Procedure

The optimization procedure is based on the approximation concept approach and is performed as follows.

1) Read input data.

2) Perform linear steady-state heat transfer analysis and calculate sensitivity of each nodal temperature. If number of variables is larger than the number of degrees of freedom, use Eq. (39); if not, use Eq. (38).

3) Perform linear static structural analysis.

4) Evaluate objective and constraint functions, determine critical retained constraint set that includes temperature and mechanical constraints.

5) Check for the design convergence.

6) Perform heat transfer sensitivity analysis.

7) Perform structural sensitivity analysis only for structural critical constraints.

8) Formulate and solve the approximate optimization problem and go to step 2.

Numerical Examples

The approximation concept and new two-point approximation methods are applied to several examples of structural optimization with temperature and strength constraints. During each approximate subproblem, DOT[35] is used as an optimizer. Because of limited references about this field, few comparisons are given.

Titanium Plate with Aluminum Bars

The titanium plate with aluminum bars shown in Fig. 1 was designed for minimum mass under temperature and stress constraints. This configuration is representative of a class of structures where one material satisfies strength requirements and the other acts as an efficient conductor to transfer incident heat to a heat sink. The sink is represented by the panel edge maintained at $T = -18°C$. Loads applied to the structure include a force per unit width N_x, shown in Fig. 1a. Two different values of N_x are used in this calculation, 210 KN/m and 6.30 MN/m. The heat load consists of a uniform heat flux 3.3 KW/m^2 over the surface of plate. Material properties, stress, and temperature limits are given in Fig. 1b. The finite element model is shown in Fig. 2 and includes 24 six-node isoparametric elements, 12 rod elements, and 61 nodes, resulting in 36 design variables. Because of symmetry, only half of the structure is modeled.

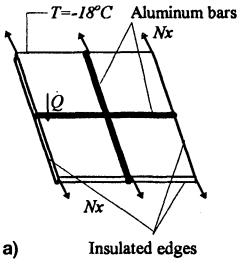

a) b)

Property	Aluminum	Titanium
ρ kg/mm^3	2.770×10^{-6}	4.437×10^{-6}
k w/mm °c	2.340×10^{-1}	9.490×10^{-3}
α °c^{-1}	2.83×10^{-5}	1.04×10^{-5}
E GPa	73.0	103
$\bar{\sigma}$ MPa	320	700
$\bar{T}$ °c	177	260

Fig. 1 Titanium plate with aluminum bars: a) configuration and loads and b) material properties. Plate dimension = 305 mm × 305 mm.

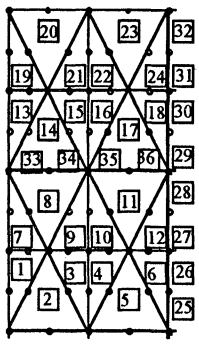

Fig. 2 Finite element method model of a titanium plate with aluminum bars, 24 six-node triangular elements and, 12 two-node rod elements with 36 variables (half model).

Table 1 Iterative histories of a titanium plate with aluminum bars

	N_x = 210 KN/m		N_x = 6.30 MN/m	
Iteration number	Objective function, kg	Maximum constraint	Objective function, kg	Maximum constraint
1	23.533	−0.884	23.533	−0.874
2	3.809	-4.886×10^{-3}	3.966	-4.021×10^{-3}
3	2.638	-2.556×10^{-2}	2.908	2.193×10^{-2}
4	2.444	3.173×10^{-2}	2.706	1.342×10^{-1}
5	2.340	4.531×10^{-2}	2.687	2.680×10^{-2}
6	2.295	3.971×10^{-2}	2.669	1.197×10^{-2}
7	2.336	3.600×10^{-3}	2.683	4.780×10^{-3}
8	2.326	-1.167×10^{-3}	——	——

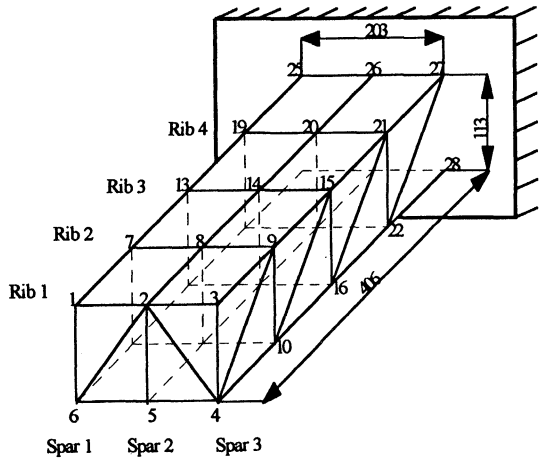

Fig. 3 Wing box configuration.

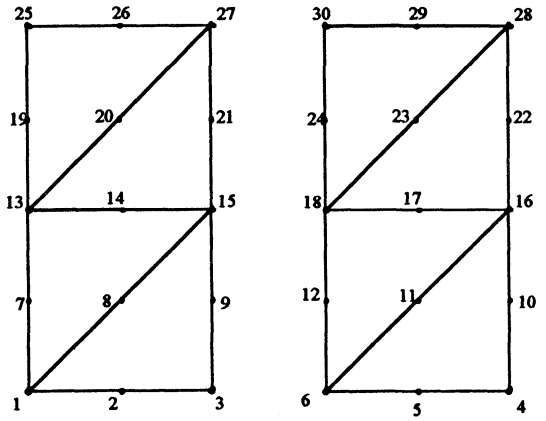

Fig. 4 Upper and lower shins (six-node element type).

For the case where N_x = 210 KN/m, the present method gives an optimum value of 2.326 kg with eight iterations. The final design is governed by the temperature constraints. None of the elements are stress-critical. Adelman et al.[12] gave an optimum mass of 2.365 kg [by the optimality criterion with fully stressed design (FSD)] or 2.360 kg (by mathematical programming-SUMT).

For the case where N_x = 6.30 MN/m, the method of this work yields the optimum mass of 2.68 kg while the optimality criterion method with FSD[12] gave 2.40 kg. The present number of iterations are 8 with 1% convergence criterion while Ref.12 took 16 iterations with 5% convergence criterion by the optimality criterion method with FSD[12]. Iterative histories are shown in Table 1 with initial areas of rod as 9290 mm^2 and thickness of the plate as 76 mm.

Wing Box

Figure 3 shows a wing box configuration. Material properties of the wing box are as follows: $\rho = 8.248 \times 10^{-3}$ kg/cm^3, $k = 1.500 \times 10^{-1}$ w/cm K, $\alpha = 1.380 \times 10^{-5}$ K^{-1}, E = 193.0 GPa. The wing box is built-in at the root and consists of upper and lower covers, four ribs, and three spars. The loading includes in-plane forces per unit length N_x, N_y, and N_{xy}, and uniform heat flux applied over the lower surface of the structure. Boundary conditions include prescribed temperatures on edges 1–4 (edges 1: node 1-2-3; edges 2: node 4-5-6; edges 3: node 25-26-27; edges 4: node 28-29-30), and prescribed zero displacements on edges 3 and 4. The thermal design requirements impose an upper limit of 1090 K on the temperature of all structural elements. The allowable stress for all structural elements is 875 MPa and minimum gauge limitations are bar areas of 0.064 cm^2 and membrane thickness of 0.0254 cm. A summary of loads, boundary conditions and other details

Table 3 Iterative history of the wing box (76 variables)

Iteration number	Solution, kg	
	Objective function	Maximum constraint
1	38.675	2.810
2	58.191	9.543×10^{-1}
3	112.04	1.480×10^{-1}
4	211.31	5.908×10^{-2}
5	391.37	1.360×10^{-2}
6	402.72	-2.497×10^{-5}
7	402.72	-2.497×10^{-5}

are given in Ref. 13. The ribs and spars are modeled by rod elements, whereas covers are modeled by membrane elements shown in Fig. 4. The model consists of 68 rod elements, eight membrane elements, and 30 nodes, resulting in an optimization problem with 76 design variables and 100 constraints. The present method yields the optimum mass as 402.7 kg in six iterations, whereas Ref. 13 obtained the final mass of 486 kg after 12 unconstrained minimizations. The convergence is tabulated in Table 2 with all initial plate thickness as 0.0254 cm and all rod areas as 0.064 cm^2.

Conclusions

Thermal structural optimization is one of the major design problems for a high-speed structural design. Temperatures are usually treated as fixed load-type quantities, which means temperatures are independent of design variables. This paper deals with structural optimization subject to combined thermal and mechanical loads and both strength and thermal constraints. The primary idea of the solution is the approximation concept combined with the newly developed two-point approximation, which can efficiently solve thermal structural optimization. Efficiency is based on the following factors:

1) Two-point approximation of the function: This two point approximation is an incomplete second-order Taylor series expansion with respect to the intervening variables with only diagonal terms of the Hessian matrix retained. The diagonal terms depend on the current state of design. Both the exponential value for each intervening variable and a parameter in the second-order term are evaluated by matching the derivatives and the approximate function with their exact correspondents at the previous point. Both approximate function and derivative values at two data points are equal to their exact counterparts. More significant is that all exponential and parameter values can be obtained in a closed form, which is computationally inexpensive to build the approximate representation.

2) Consideration of coupling between the heat transfer and the structural analysis: Coupling between the heat transfer and the structural analysis is taken into account. This coupling includes both temperature and its derivative effects on structural responses and its derivatives.

3) Approximation of the internal forces instead of stresses: The stress constraints are very sensitive with the respect to design variables. Internal force is relatively stable with the change of variables. The internal forces are approximated first at the interested points, then the stress is calculated using the approximated forces.

In summary, the example problems demonstrated the robustness of the new-point approximation for the design of thermal structures.

Acknowledgment

This research work has been sponsored by U.S. Air Force through Contract F33615-94-C-3211.

References

[1]Thornton, E. A., *Thermal Structures for Aerospace Application*, AIAA Education Series, AIAA, Reston, VA, 1996.

[2]Meric, R. A., "Boundary Element in Shape Sensitivity Analysis

of Thermoelastic Solids,'' *NATO Advanced Study Institute Series, Computer Optimal Design: Structural and Mechanical System*, edited by C. A. Mota Soars, Springer–Verlag, Berlin, 1987, pp. 643–652.

[3]Aithal, R., and Saigal, S., "Shape Sensitivity Analysis in Thermal Problems Using BEM,'' *Engineering Analysis with Boundary Elements*, Vol. 15, No. 2, 1995, pp. 115–120.

[4]Dems, K., "Sensitivity Analysis in Thermoelasticity Problems,'' *NATO Advanced Study Institute Series, Computer Optimal Design: Structural and Mechanical System*, edited by C. A. Mota Soars, Springer–Verlag, Berlin, 1987, pp. 563–572.

[5]Hou, G., Sheen, J. S., and Chuang, C. H., "Shape Sensitivity Analysis and Design Optimization of Linear, Thermoelastic Solids,'' *Proceedings of the AIAA/ASME/ASCE/AHS/ASC 31st Structures, Structural Dynamics, and Materials Conference* (Long Beach, CA), AIAA, Washington, DC, 1990, pp. 206–216.

[6]Yang, R. J., "Shape Design Sensitivity Analysis of Thermoelasticity Problems,'' *Computer Methods in Applied Mechanics and Engineering*, Vol. 102, No. 1, 1993, pp. 41–60.

[7]Tortorelli, D. A., Haber, R. B., and Lu, S. C. Y., "Adjoint Sensitivity Analysis for Nonlinear Dynamics Thermoelastic Systems,'' *AIAA Journal*, Vol. 29, No. 2, 1991, pp. 253–263.

[8]Pangiotis, M., and Tortorelli, D. A., "Analysis and Optimization of Weakly Coupled Thermoelastic Systems with Applications to Weldment Design,'' *International Journal for Numerical Methods in Engineering*, Vol. 38, No. 8, 1995, pp. 1259–1285.

[9]Haftka, R. T., and Markus, D. S., "Techniques for Thermal Sensitivity Analysis,'' *International Journal for Numerical Methods in Engineering*, Vol. 17, No. 1, 1981, pp. 17–80.

[10]Haftka, R. T., and Markus, D. S., "Calculation of Sensitivity Derivatives in Thermal Problems by Finite Differences,'' *International Journal for Numerical Methods in Engineering*, Vol. 17, No. 12, 1981, pp. 1811–1821.

[11]Kodiyalam, S., and Parthasarathy, V. N., "Ply Layout Optimization and Micromechanics Tailoring of Composite Aircraft Engine Structures,'' *Journal of Propulsion and Power*, Vol. 10, No. 6, 1994, pp. 897–905.

[12]Adelman, H. M., Sawer, P. L., and Shore, C. P., "Optimum Design of Structures at Elevated Temperatures,'' *AIAA Journal*, Vol. 17, No. 6, 1979, pp. 622–629.

[13]Adelman, H. M., and Sawyer, P. L., "Inclusion of Explicit Thermal Requirements in Optimum Structural Design,'' NASA TM X-74017, March 1977.

[14]Haftka, R. T., and Shore, C. P., "Approximation Methods for Combined Thermal/Structural Design,'' NASA TP 1428, June 1978.

[15]Haftka, R. T., "Design for Temperature and Thermal Buckling Constraints Employing Noneigenvalue Formulation,'' *Journal of Spacecraft*, Vol. 20, No. 4, 1983, pp. 363–367.

[16]Thomas, H. L., and Shyy, Y.-K., "Optimization of Structures with Static and Thermal Loads,'' *Proceedings of the AIAA/ASME/ASCE/AHS/ASC 34th Structures, Structural Dynamics, and Materials Conference*, (La Jolla, CA), 1993, pp. 1438–1442.

[17]Cheu, T., "Sensitivity Analysis and Shape Optimization of Axisymmetric Structures,'' *International Journal for Numerical Methods in Engineering*, Vol. 28, No. 1, 1989, pp. 95–108.

[18]Cheu, T., "Procedures for Shape Optimization of Gas Turbine Disks,'' *Computers and Structures*, Vol. 34, No. 1, 1990, pp. 1–4.

[19]Hattori, T., and Ohnishi, H., "Optimum Design of Rotational Wheels Under Transient Thermal and Centrifugal Loading,'' *JSME, International Journal*, Series III, Vol. 32, No. 4, 1989, pp. 597–605.

[20]Shao, M., and Guan, Z., "Process Optimization of Transient Thermal Stress Field,'' *International Journal of Pressure Vessels and Piping*, Vol. 58, No. 3, 1994, pp. 303–308.

[21]Ke, J., "Rule-Based Shape Optimization of Disks Subjected to Transient Thermoelastic Loading,'' *Journal of Mechanical Design*, Vol. 116, No. 2, 1994, pp. 419–422.

[22]Autio, M., "Coupled Thermal-Structural Problems in the Optimization of Laminated Plates,'' *Structural Optimization*, Vol. 15, No. 1, 1998, pp. 49–56.

[23]Narayanan, G. V., Reddy, E. S., Abumeri, G., Hopkins, D. A., and Chamis, C. C., "Structural Tailoring/Analysis for Hypersonic Components: A Computational Simulation,'' *Proceedings of the AIAA/USAF/NASA/OAI 4th Symposium on Multidisciplinary Analysis and Optimization* (Cleveland, OH), AIAA, Washington, DC, 1992, pp. 251–262.

[24]Stubbe, J., "PAYCOS: A Multidisciplinary Design Optimization Tool for Hypersonic Vehicle Design,'' *Proceedings of the AIAA/USAF/NASA/OAI 4th Symposium on Multidisciplinary Analysis and Optimization* (Cleveland, OH), AIAA, Washington, DC, 1992, pp. 263–271.

[25]Hwang, Y., and Vanderplaats, G. N., "Generalized Multidisciplinary Optimal Design Tool for Windows Based Computer Platforms,'' *Proceedings of the AIAA/NASA/USAF/ISSMO 5th Symposium on Multidisciplinary Analysis and Optimization* (Panama City, FL), AIAA, Washington, DC, 1994, pp. 1085–1090.

[26]Zhang, J., "Modified Thermal Load Approach for Automatic Generation of Basis Vector in Shape Optimization,'' *Proceedings of the AIAA/NASA/USAF/ISSMO 5th Symposium on Multidisciplinary Analysis and Optimization* (Panama City, FL), AIAA, Washington, DC, 1994, pp. 384–390.

[27]Narayan, J. R., Chattopadhyay, A., Pagaldipti, N., and Zhang, S., "Integrated Aerodynamics and Heat Transfer Optimization Procedure for Turbine Blade Design,'' *Proceedings of the AIAA/ASME/ASCE/AHS/ASC 36th Structures, Structural Dynamics, and Materials Conference* (New Orleans, LA), AIAA, Washington, DC, 1995, pp. 2973–2982.

[28]Chamis, C. C., "Infrastructure for Coupled Multidisciplinary Problems in Engine Structures,'' *Proceedings of the AIAA/NASA/USAF/ISSMO 6th Symposium on Multidisciplinary Analysis and Optimization* (Bellevue, WA), AIAA, Washington, DC, 1996, pp. 1409–1419.

[29]Tappeta, R., Nagaendra, S., and Renaud, J. E., "A Multidisciplinary Design Optimization Approach for High Temperature Aircraft Engine Components,'' *Proceedings of the AIAA/ASME/ASCE/AHS/ASC 39th Structures, Structural Dynamics, and Materials Conference* (Long Beach, CA), AIAA, Reston, VA, 1998, pp. 1055–1065.

[30]*ASTROS User's Manual, Version 20.0*, Universal Analytics, Inc., Torrance, CA, 1997.

[31]Vanderplaats, G. N., and Miura, H., "GENESIS—Structural Synthesis Software Using Advanced Approximation Techniques,'' *Proceedings of the AIAA/USAF/NASA/OAI 4th Symposium on Multidisciplinary Analysis and Optimization* (Cleveland, OH), AIAA, Washington, DC, 1992, pp. 180–190.

[32]Xu, S., and Grandhi, R., "An Effective Two-Point Function Approximation for Design Optimization,'' *Proceedings of the AIAA/ASME/ASCE/AHS/ASC 39th Structures, Structural Dynamics, and Materials Conference* (Long Beach, CA), AIAA, Reston, VA, 1998, pp. 2181–2191.

[33]Wang, L. P., and Grandhi, R. V., "Improved Two-Point Function Approximation for Design Optimization,'' *AIAA Journal*, Vol. 33, No. 9, 1995, pp. 1720–1727.

[34]Wang, L., and Grandhi, R. V., "Multipoint Approximations: Comparisons Using Structural Size, Configuration and Shape Design,'' *Structural Optimization*, Vol. 12, No. 2–3, 1996, pp. 177–185.

[35]*DOT Users Manual, Version 4.2*, Vanderplaats Research & Development, Inc., Colorado Springs, CO, 1995.